ISSN: 0067-2904

Determine the Radon Gas Level Using the GIS Technique for Baghdad City

Mustafa Ali Hassan[1], Ola Adil Ibrahim[*2]
[1]Remote Sensing Unit, College of Science, University of Baghdad, Baghdad, Iraq.
[2]Department of Physics, College of Science, University of Baghdad, Baghdad, Iraq.

Abstract

In this work, radon concentrations in the polluted environment were measured within the Baghdad sample surface soil conservation, and this was done using a RAD-7 mobile detector. The work consists of four parts:

The first part includes calculating the latitude and longitude of each point of the study area using the Global Positioning System (GPS). The second part of which includes Determination of 222Rn gas concentrations in surface soil samples. In the northeast part of Baghdad, the highest concentration of radon was found in Al-Shaab area (3.11 ±175.33 Bq / m^3), while the lowest gas concentration in AL Gzeera area (6.67±73.00 Bq/ m^3), In the northwest part of Baghdad, the highest concentration of radon was found in the al-Taji area (4.22 ± 179.33Bq / m^3) and the lowest concentration of Radon gas in Al Ghazaliya area (3.11 ± 68.33 Bq/ m^3). In the southeast part of Baghdad, the highest concentration of radon was found in AL-Wahda area (1.78 ±175. 33Bq / m^3) while the lowest rate of radon gas is located in the Karada area (1.78 ± 41.67Bq / m^3). The highest concentration of radon gas can be observed in the southwest part of Baghdad in Mahmudiya area (4.22 ± 185.67Bq/m3), while the lowest concentration of radon in Aamiriya (2.22 ± 78.67Bq/m^3). The third part includes the applied the techniques of interpolation using the radon data available in the known sites to estimate the radon data for the non-measured area, which will help to develop an effective plan to reduce the concentration of radon in the study area. The fourth part includes the preparation of a soil surface classification map in all selected areas where the soil was classified into five species using the Erdas2014.

Keywords: Radon gas, RAD-7, Remote sensing, Baghdad city, Band ratios.

تحديد مستوى غاز الرادون باستخدام تقنية نظم المعلومات الجغرافية لمدينة بغداد

مصطفى علي حسن[1]، علا عادل ابراهيم[*2]
[1]وحدة الاستشعارعن بعد، كلية العلوم، جامعة بغداد، بغداد، العراق.
[2]قسم الفيزياء، كلية العلوم، جامعة بغداد، بغداد، العراق.

الخلاصة

في هذا العمل، تم قياس تراكيز غاز الرادون في التربه السطحيه للعاصمه بغداد ،و ذلك باستخدام جهاز RAD−7. اذ يتألف العمل من أربعة أجزاء: الجزء الأول حساب خطوط الطول والعرض لكل نقطة مختاره من منطقة الدراسة باستخدام النظام العالمي لتحديد المواقع (GPS). ويشمل الجزء الثاني حساب تراكيز غاز 222Rn في عينات التربة السطحية وكانت النتائج كما يلي: في الجزء الشمالي الشرقي من بغداد وجد ان

*Email: oula2486@yahoo.com

أعلى معدل لتركيز غاز الرادون كان في منطقة الشعب ($175.33Bq/m^3$±3.11)، في حين تسجيل أدنى معدل لتركيز غاز الرادون في منطقة الجزيرة ($73.00Bq/m^3$±6.67)، اما في الجزء الشمالي الغربي من بغداد وجد ان أعلى معدل لتركيز غاز الرادون كان في منطقة التاجي ($179.33Bq/m^3$±4.22) وسجل أدنى معدل تركيزغاز الرادون في منطقة الغزالية ($68.33Bq/m^3$±3.11) اما في الجزء الجنوبي الشرقي من بغداد وجد ان أعلى معدل لتركيز غاز الرادون في منطقة الوحدة ($175.33Bq/m^3$ ± 1.78) في حين كان أدنى معدل لتركيز غاز الرادون في منطقة الكرادة ($41.67Bq/m^3$±1.78), و يمكن ملاحظه اعلى تراكيز غاز الرادون في الجزء الجنوبي الغربي من بغداد في منطقة المحمودية ($185.67Bq/m^3$±4.22) في حين وجد أدنى معدل لتركيز الرادون في منطقه العامريه ($78.67Bq/m^3$±2.22). اما الجزء الثالث يمثل تطبيق تقنيات الأستيفاء المكاني باستخدام بيانات غاز الرادون المتاحة في المواقع المعروفة لتقدير بيانات غاز الرادون للمناطق غير المقاسة مما سيساعد على وضع خطة فعالة للحد من تركيز غاز الرادون في منطقة الدراسة. ويتضمن الجزء الرابع إعداد خريطة لتصنيف سطح التربة في جميع المناطق المختارة حيث تم تصنيف التربة إلى خمسة أنواع باستخدام برنامج ERDAS2014.

Introduction

Geographic information system (GIS) technologies include GPS (global positioning system), RS (remote sensing), and capabilities for input, storage, and manipulation (or analysis) and output of geographic information, It can be defined GIS as a system for capturing, checking, integrating, manipulating, analyzing, and displaying data which are spatially referenced to the Earth [1]. It is an assemblage of hardware and software that becomes useful only when it is properly placed in an organization and supported by expertise, structured data, and organizational routines. Remote sensing is defined as the science an art of getting information about an object, phenomenon, or area through the analysis of data obtained by a device without connection with the area, object or phenomena under investigation. Remote sensing is based on the analysis of the Interaction between a flow of electromagnetic radiation and the phenomena or object under investigation, [2]. Remote sensing is revealed as a successful tool for mapping background levels of soil heavy metals and accurate delineation of polluted areas, [3]. Radon 222Rn a naturally occurring radioactive, inert gas (half-life of 3.8 days) [4]. Radon was the fifth radioactive element to be discovered, in 1900 by Friedrich Ernst Dorn. After uranium, thorium, radium and polonium, In 1900 Dorn reported some experiments in which he noticed that radium compounds emanate a radioactive gas he named Radium Emanation (Ra Em), [5]. In many countries, radon is the second most important cause of lung cancer after smoking, the proportion of lung cancers attributable to radon is estimated to range from 3 to 14% significant health effects have been seen in uranium miners who are exposed to high levels of radon, [6]. The radon gas formed in the soil emanates and diffuses through the Pore spaces of the soil matrix. The degree of emanation depends on allocation of 226Ra in soil and many geophysical parameters like diffusion porosity, permeability and meteorological parameters like pressure and temperature, Radon can also emigrate by convection mechanism through pore spaces in the soil, fractures in the rocks and along with weak zonessuchasshear, faults thrust, etc., [7].

The Study area

Baghdad is the capital city of Iraq and it is located on a wide plain bisected by the river Tigris Figure-1. The Tigris has divided the Baghdad city approximately in half, with the eastern half being called Al-Rusafa and the Western half known as Al-Karkh. Lies between latitudes 33.452, 33.184° N, and longitudes 44.189, 44.576° E, [8]. Is located nearly (32 m) above the sea level, with a total area of Baghdad city about (4555 km^2) The region has a hot and dry climate in the summer and a mild climate to cool in the spring and winter Areas, [9].

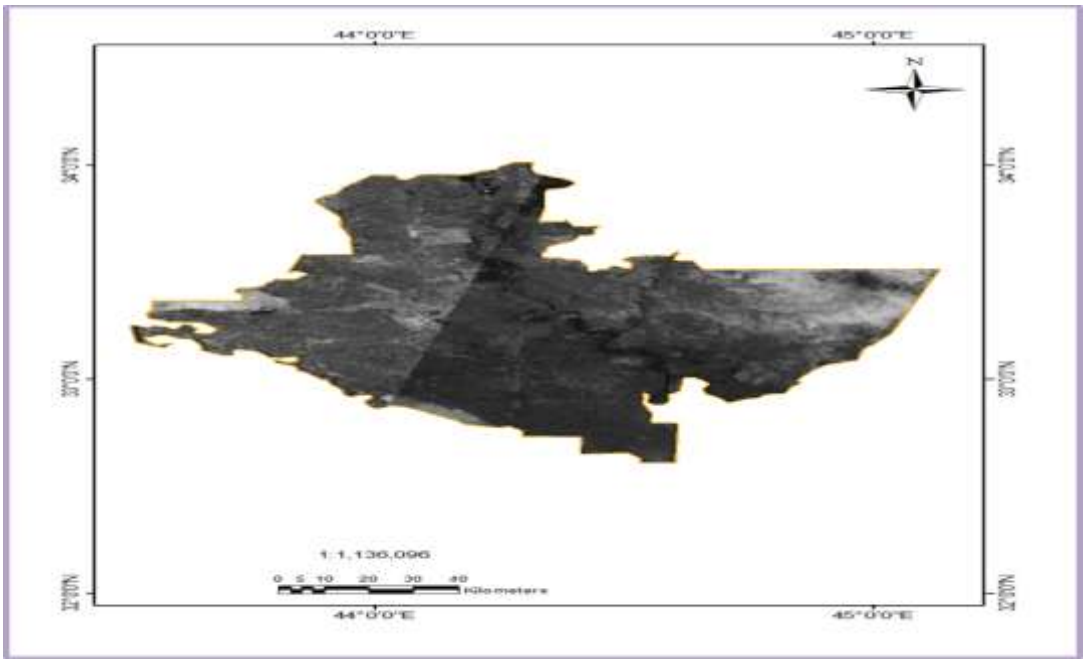

Figure1-Baghdad capital of Iraq.

Analysis of data measurement for Radon concentrated of soil

In this work, radon concentration in surface soil was measured using RAD-7 in different locations in Baghdad. Current results in the study area showed that radon concentrations in surface soil samples were below the recommended value (200Bq / m^3), [10]. All sample periods of measurements were during the months (December, January, February 2016, 2017).

Table-1shows the concentration of radon in the surface soil of Baghdad governorate in addition to the latitude and longitude of the selected areas of the study area. Using the Arc. Map 9.3 programs; a map was drawn showing radon concentrations as shown in Figure-2. Spatial interpolation is widely used for creating continuous data when data are collected at discrete locations In this work has been selected as the reverse weighting method (IDW) as shown in Figure-3.

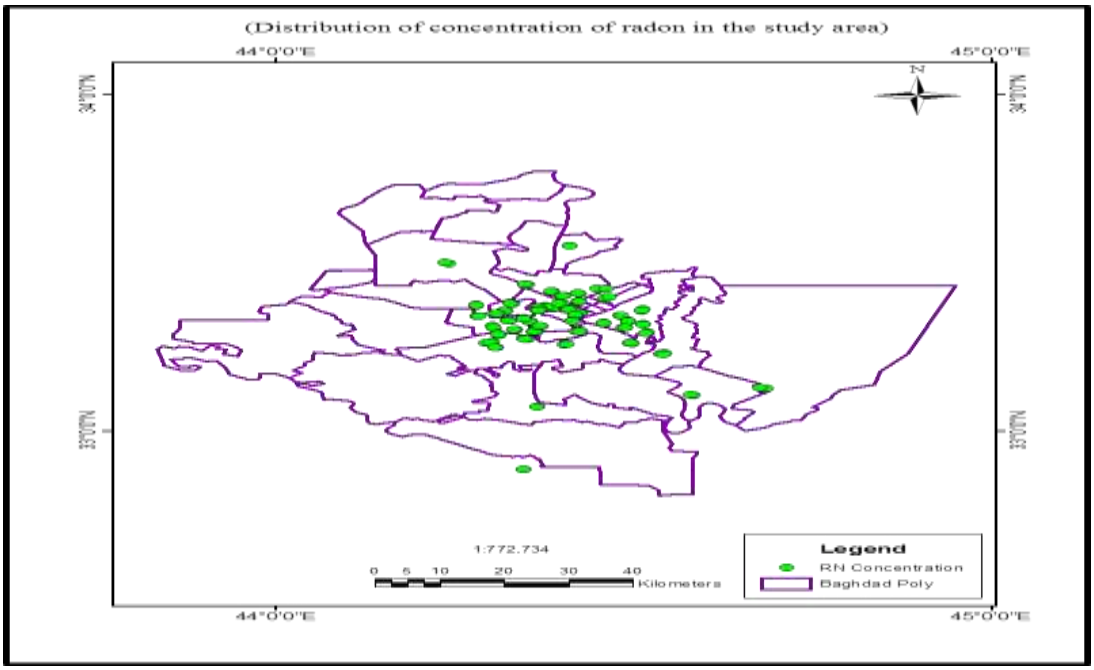

Figure 2-Distribution of radon concentration for each province of Baghdad.

Table 1- shows latitude and longitude for all samples taken in this study In addition to radon concentrations in the same area.

NO.	Radon location name	X-axis pixel	Y-axis pixel	RN. CO.	Mean of **C.** RN (Bq/m^3)
1	Shaab	442690.17 442855.416 442754.257	3697217.97 3697274.533 3697095.717	175 180 171	175.33
2	AL Gzeera	439403.45 439404.436 439696.789	3699591.17 3699392.615 3699489.172	77 79 63	73.00
3	Taji	428956.55 428568.317 429549.677	3706823.62 3706422.078 3706439.057	173 180 185	179.33
4	al ghazaliya	433175.62 433059.096 433149.307	3689122.58 3689045.797 3689234.063	67 65 73	68.33
5	Wahda	470267.48 470708.109 469718.292	3665215.67 3665069.571 3665344.998	175 178 173	175.33
6	Al karada	446236.179 445990.763 446452.582	3683991.798 3683895.464 3684078.948	44 42 39	41.67
7	Aamiriya	435087.147 435003.148 435250.902	3685379.895 3685854.89 3685123.57	77 77 82	78.67
8	Mahmudiyah	440754.83 440755.299 440731.524	3659262.97 3659240.229 3659283.897	181 184 192	185.67

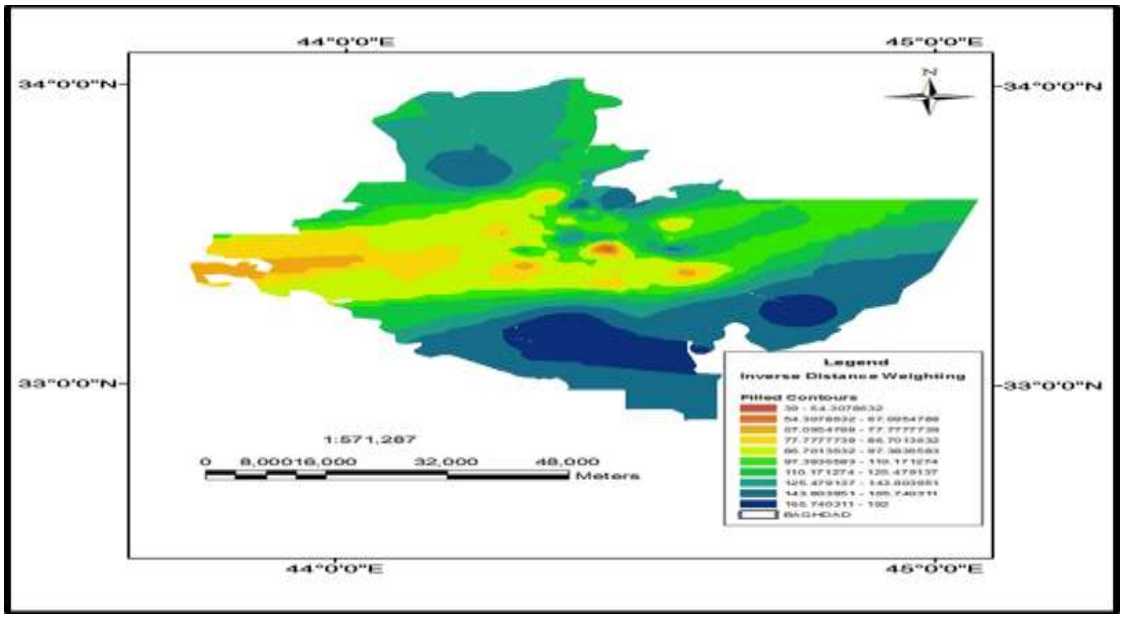

Figure 3-interpolation of Radon concentration in Soil using IDW method.

Band ratios

The use of ASTER multispectral data in mineral exploration and lithological mapping has increased in recent years due to spectral characteristics of unique, integral, ASTER bands are highly sensitive to hydrothermal alteration minerals, especially in shortwave infrared radiation SWIR region and the possibility of applying the diversity of image processing techniques, 'on-demand' data

availability with low cost and broad coverage for regional scale mapping. ASTER has a total of 14 spectral channels; but with the spectral ratioing among these selective bands, more lithologic and mineralogic indices and more accurate results can be derived from ASTER image, defined vegetation index and mineralogic indices for visible and near infrared radiation ASTER VNIR and SWIR bands and lithologic indices for ASTER thermal infrared radiation TIR bands with considering spectral absorption features of vegetation and different minerals and rocks in ASTER spectral channels, these indices are listed as follows,[11] ,[12].

Kaolinite Index (KLI) = $[\frac{Band4}{Band5}]$ $[\frac{Band8}{Band6}]$

Calcite Index (CLI) = $[\frac{Band6}{Band8}]$ $[\frac{Band9}{Band8}]$

Dolomite = $\frac{(6+8)}{7}$

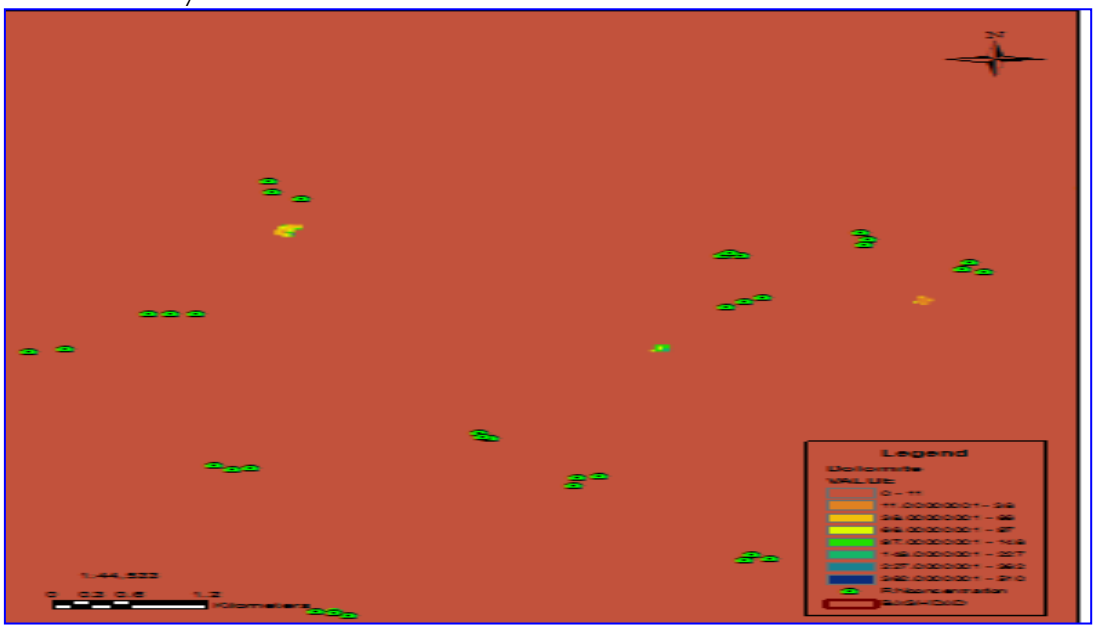

Figure 4(a)-the image shows an increase in the amount of dolomite with increased concentration of radon the formula was [band6+band8 / band7], [12].

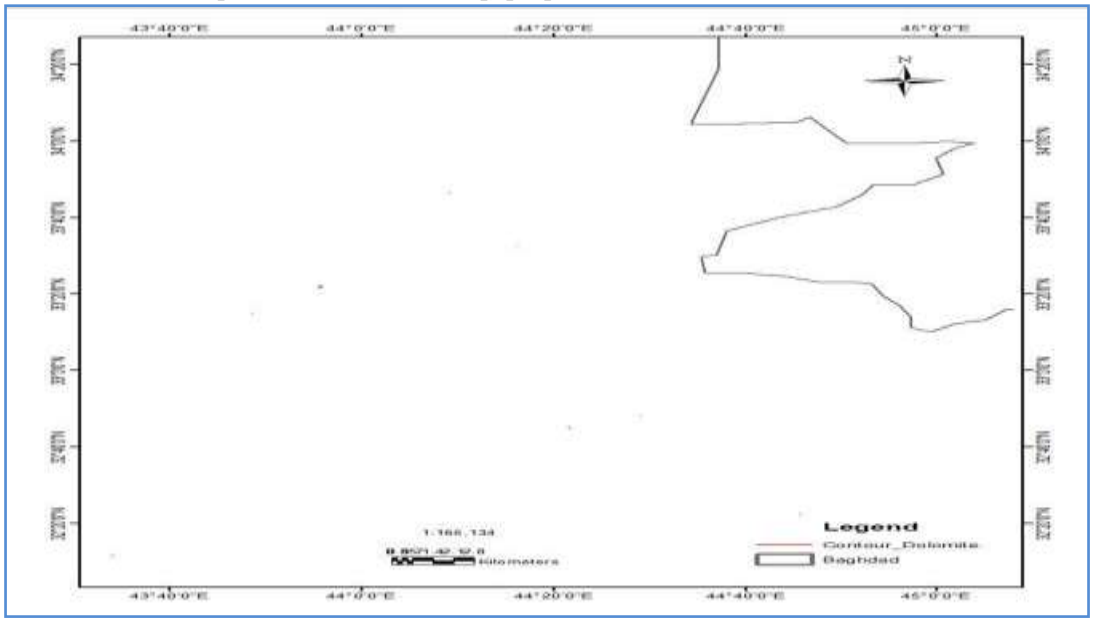

Figure 4(b)-represents the contour of dolomite after applied band ratio.

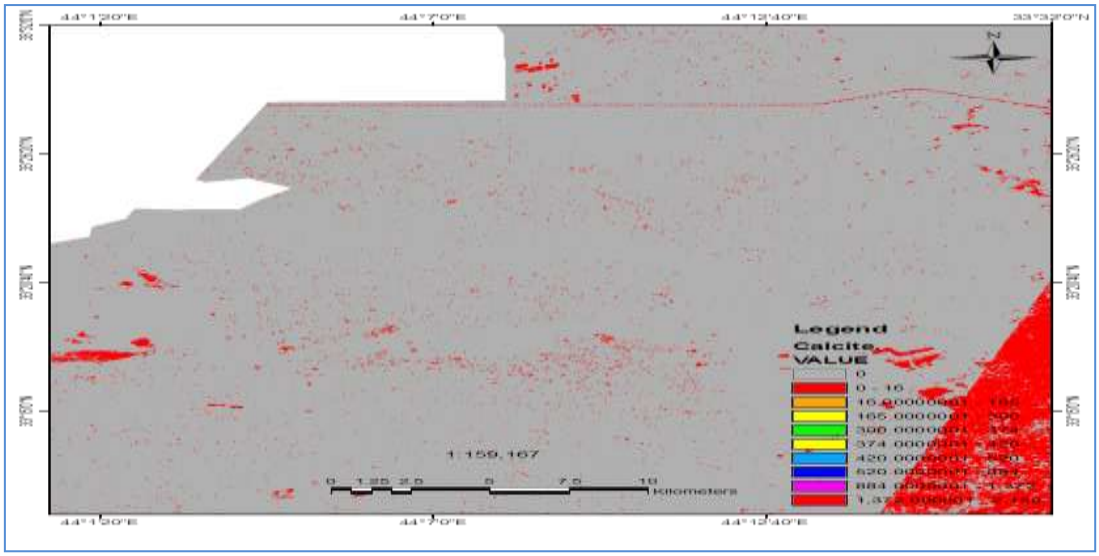

Figure 5(a)-The image shows the presence of calcite, the formula was [band6 /band8] [band9/band8] [11].

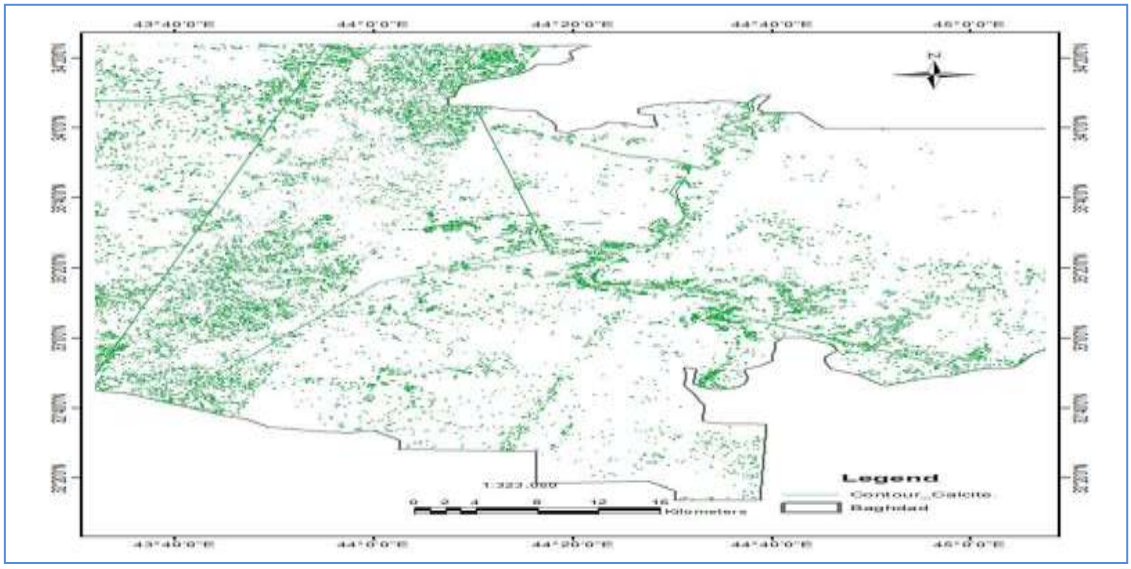

Figure 5(b)-represents the contour of calcite after applied band ratio.

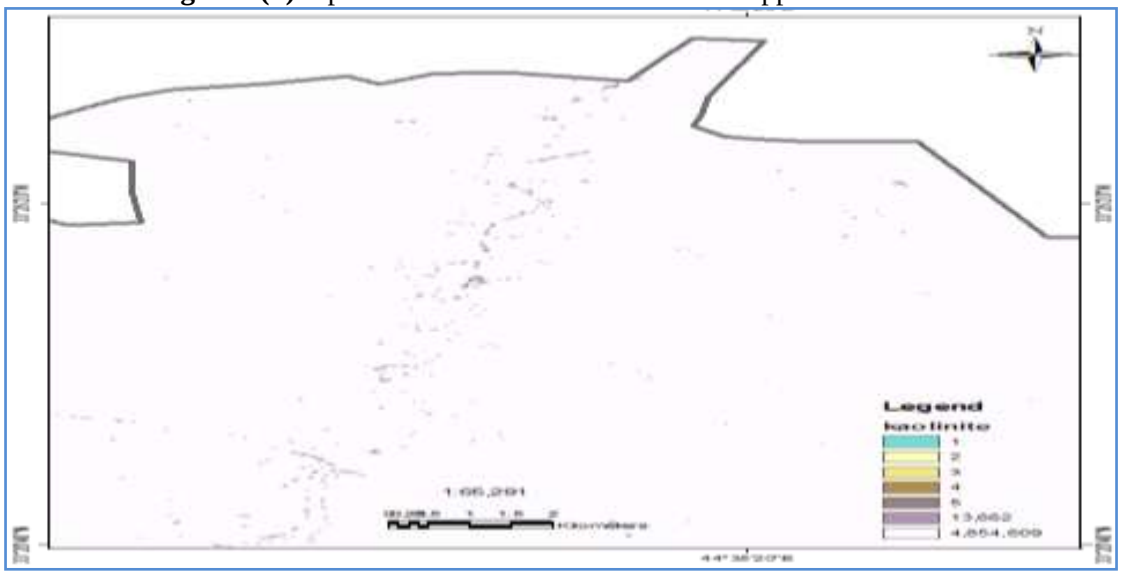

Figure 6(a)-the Kaolinite can is observed at varying rates depending on the geological characteristics of the area. The formula was [band4 /band5] [band8 /band6], [11].

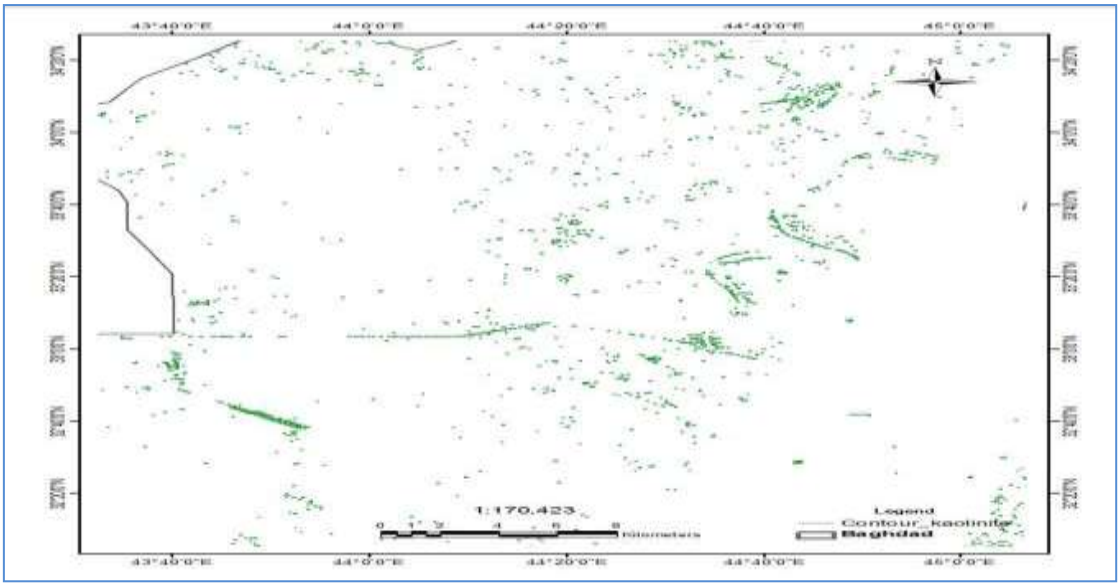

Figure 6(b)-represents the contour of Kaolinite after applied band ratio.

Classification the Satellite Image

Classification is a process aimed at dividing the satellite image into a number of categories or groups to represent each category, including a specific geographical phenomenon on the Earth's surface. The classification process depends on the nature of the area (urban, desert or mountainous, agriculture, etc.) and spatial resolution and the radiological resolution of the used satellite. There are two types of classification of non-controlled classification, under supervision.

In this study the selection method was chosen under the supervision of requiring input from the analyst, the input of the analyst, known as the training group, the training sample is the most important factor in the satellite image classification methods under supervision, the accuracy of the methods and depends largely on the samples taken for training and training Samples are two types, one used for classification and another to supervise classification accuracy, and different classification techniques deal with different types of similarity matching methods. The supervised classification includes additional functions such as analysis of input data, creation of training samples and signature files, identification of the quality of training samples and signature files, [13].

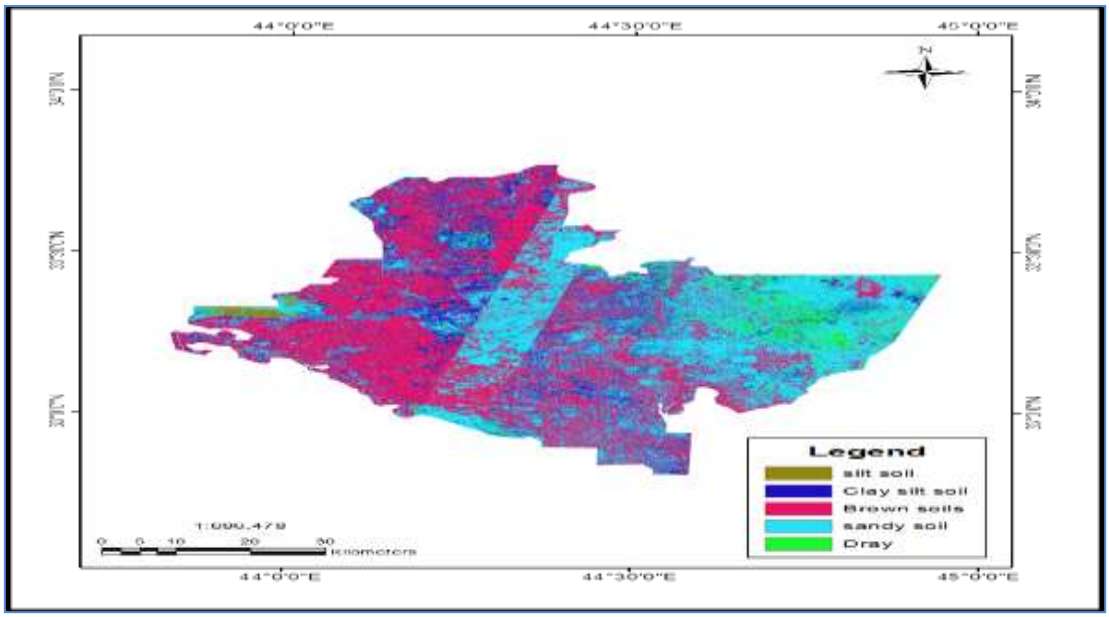

Figure 7-shows the Image of the near space of visible light and was classified into five groups of (silt, clay silt, Brown, sandy, Dray) of soil.

Table 2-represents information on areas classified into five different types of soils.

No.	Class name	Total area km^2
1	Silt soil	25.3
2	Clay silt soil	606.8
3	Brown soil	1870.4
4	Sandy soil	1903.0
5	Dry soils	149.6
Total area		4555

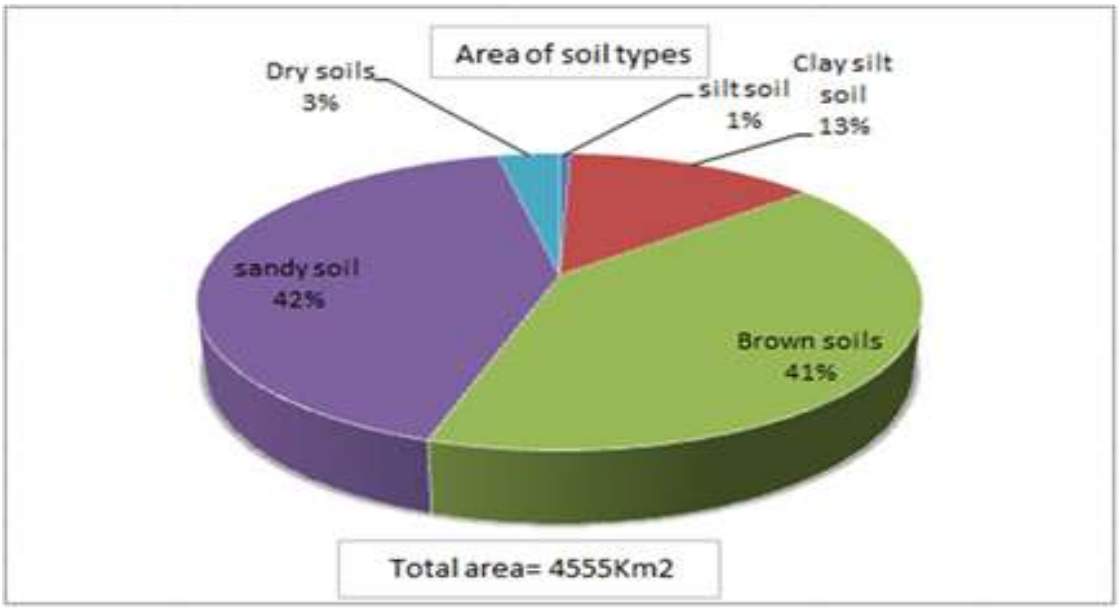

Figure 8-shows the percentage of soil types classified for Baghdad.

Results and Discussion

In this study, the radon gas concentrations were measured in surface soil using the RAD-7 detector Table-1. Shows the Radon gas concentrations in surface soil samples in the Baghdad, radon concentrations increase with the presence of calcite, dolomite and Kaolinit shows Figure-4(a, b). Figure-5(a, b), Figure-6(a, b), the reason for the increased concentration of radon is that, (AL-Shaab) area lies within the boundaries of the oil fields, located east of Baghdad. In addition to the abundance of the calcite stone which, the reason for the increased concentration of the Radon in the samples of surface soil is that the area of (AL-Wahda) because these samples are taken from areas within the limits of the Atomic Energy Organization located south of Baghdad, The reason for the increased concentration of Radon gas in surface soil samples is that the area of (AL-Taji) is considered to be an agricultural area, brown soil contains a high proportion of organic matter has been found a relationship between the concentration of radon with the presence of this type of soil as the concentrations of radon increase with the presence of brown soil in the study area.

Conclusions

The results have shown that the average of the Radon gas concentrations in the surface soil samples is less than the recommended value, given by the (ICRP, 1993). Radon concentration increases with the presence of calcite and dolomite, increased radon concentrations with kaolin; radon is increasingly concentrated in areas hit by military bombardment during the war, radon concentrations increase in agricultural soil due to the use of chemical fertilizers. It is also known that fertilizers contain uranium ratios High.

Reference

1. Chapter 14 in Bolstad, Paul. **2005**. *GIS Fundamentals, A First Text on Geographic Information Systems*", 2nd. Ed. White Bear Lake, MN: Eider Press.

2. Choudhury, E.S. and Das, E.S. **2012**. GIS and Remote Sensing For Landfill Site Selection- A Case Study on Dharmanagar Nagar Panchayet, **1**(2): 36–43.

3. Melendez-pastor J. Navarro-Pedreño , I. Gómez, and M.B. Almendro-Candel., **2011.** The Use of Remote Sensing to locate Heavy Metal as Source of Pollution. *Advances in Environmental Research*, **7**: 225-233.

4. Parajuli, P., Thapa, D. and Shah, B.R. **2015**. Study of Radon Exhalation Rate in Soil Samples of Kathmandu Valley Using Passive Detector LR115, *Int. J. Chem. Phys. SCI*., **4**(4): 30–39.

5. Krebs E Robert. **2006**. *The history and use of our earth's chemical elements: a reference guide,* 2nd Ee, Westport, Conn: Greenwood Press.

6. Krewski, D., Lubin, J.H., Zielinski, M., Alavanja, M., Catalan, V.S., William Field, R., Klotz, J.B., Le´tourneau, E.G., Lynch, F., Joseph I., Lyon, Dale P., Sandler, J. B., Schoenberg Steck, D.J., Stolwijk, J.A., Weinberg, C. and Wilcox, H.B. **2005**. Residential Radon and Risk of Lung Cancer: A Combined Analysis of 7 North American Case-Control Studies. Epidem.; National Center for Biotechnology Information, U.S. National Library of Medicine 16 (137-145).

7. Jayasheelan, M. S. S., Umeshareddy, J.K. and Ningappa, C. **2013**. Radon concentration in atmosphere and its variation with depth of the soil in and around Tumkur, Karnataka, India, *International Journal of Advanced Scientific and Technical Research*, **2**(3): 158–162.

8. Israa, J., Muhsin, Ebtesam F., Khanjer, Ban A., Abas, B., Sabah, Rafah R. **2017**. 3D Building Reconstruction Using DEM and Mosaic Model, *Iraqi Journal of Science*, **58**(3A): 1308-1316.

9. Tawfiq, N.F., Mansour, H.L. and Karim, M.S. **2015**. Measurement of Radon Gas Concentrations in Tap Water for Baghdad Governorate by Using Nuclear Track Detector (CR-39), *International Journal of Physics*, **3**(6): 233–238.

10. (ICRP), **1993**. International Commission on Radiological Protection against Radon-222 at Home and Work, Publication 65, *Pergamon, Elsevier*, 35, 242.

11. Pour, B. and Hashim, M. **2011**, Application of advanced spaceborne thermal emission and reflection radiometer (ASTER) data in geological mapping, *Int. J. Phys. SCI.*, **633**: 7657–7668.

12. Freek, D., van der Meer, Harald M.A., van der Werff, Frank J.A., van Ruitenbeek, Chris, A. Hecker,Wim H. Bakker, Marleen F. Noomen, Mark van der Meijde, E. John M. Carranza, J. Boudewijn de Smeth, Tsehaie Woldai**, 2012**. Multi- and hyperspectral geologic remote sensing: A review, *Int. J. Appl. Earth Obs. Geoinf*., **14**(1): 112–128.

13. Joana Margarida de Almeida Simoes, **2006.** An Agent-Based Approach to Spatial Epidemics through GIS, M.Sc, University of London.